Tomographic Inspection of Fiber Coils Using Optical Coherence Tomography

Zhihong Li, Zhuo Meng, Longzhi Wang, Tiegen Liu, and Steve X. Yao

***Abstract*— We report the first study of using optical coherence tomography (OCT) to inspect the winding quality of fiber optical gyro coils. We use a swept-source OCT system to scan a quadrupole-wind fiber coil for obtaining its two-dimensional and three-dimensional (3D) tomographic images. The defects beneath the surface of the fiber coil, which otherwise are invisible by video inspection, can be clearly identified with such tomographic images. The winding quality of each layer can also be independently visualized with the reconstructed 3D images from different angles or in different sections. We believe that the proposed method will be useful to ensuring the quality production of each and every fiber gyro coil.**

***Index Terms*— Optical coherence tomography, fiber-optic gyroscope (FOG), quadrupole gyros coil.**

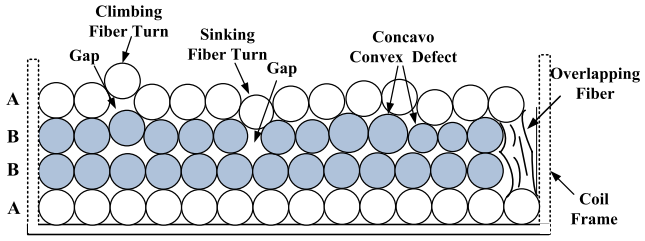

Fig. 1. Illustration of different winding defects in a quadrupole wound fiber coil, where fiber from two different supply spools labeled A and B are wound alternatively on the coil spool with the pattern ABBA, ABBA, and etc., starting from the center between spools A and B.

I. Introduction

A FIBER coil is a key component in a fiber optic gyroscope (FOG) for the precision detection of rotation rate and angle based on the Sagnac effect [1]. The fiber coil must be wound carefully with special geometries [2]–[5], such as quadrupole winding pattern, to reduce a nonreciprocal effect caused by thermal variations known as Shupe effect [6]. The winding quality of the fiber coil directly affects the performance of the FOG. Despite a large amount of FOGs have been produced for various applications, the making of quality fiber coils consistently is still a challenge, with large variations in performance for coils made with even the same process, mainly due to the inability of effective quality inspection [7].

In a perfect fiber coil, each fiber turn lays right next to the adjacent turn, as shown with the bottom two layers in Fig. 1. In addition, each fiber layer is perfectly flat with no bumps and humps. However, the following winding errors illustrate in Fig.1 are commonly found in fiber coils [8], [9]: (1) Fiber climbing, that a fiber turn climbs above its current layer, caused by pressure from its neighboring fiber turns. (2) Fiber sinking, that a fiber sinks down from its current layer, caused by inconsistent fiber winding tension. (3) Fiber gapping, that two or more fiber turns settle incorrectly from its proper positions. (4) Concavo-convex defect of the fiber layer, mainly caused by the irregularity of the fiber diameter. (5) Fiber overlapping, which often occurs at both ends of the coil when the fiber turn transitions from a lower layer to an upper layer during winding process.

These defects are more or less present in a final fiber coil product and compromise the performance of a resulting FOG, such as the bias stability and the rate or angular errors caused by thermal variation and mechanical vibrations. Therefore it is important to evaluate the quality of fiber coils, during the winding process and in the finished product, to ensure high quality production.

Video inspection with CCD cameras is commonly used to monitor the winding of a fiber coil, however it only provides surface images and is difficult to identify the defects and

Manuscript received November 15, 2014; revised December 11, 2014; accepted December 17, 2014. Date of publication December 19, 2014; date of current version February 11, 2015. This work was supported in part by the Medical Instruments and New Medicine Program of Suzhou under Grant ZXY2012026, in part by the International Science and Technology Cooperation Program of China under Grant 2009DFB10080 and Grant 2010DFB13180, in part by the National Instrumentation Program under Grant 2013YQ03015, in part by the National Basic Research Program (973 Program) of China under Grant 2010CB327806, in part by the China Post-Doctoral Science Foundation under Grant 20100470782, in part by the Foundation Research Project of Jiangsu Province under Grant BK20130374 and Grant BK20130373. *(Corresponding author: Zhuo Meng.)*

Z. Li is with the Key Laboratory of Optoelectronics Information Technology Polarization Research Center, College of Precision Instrument and Optoelectronics Engineering, Ministry of Education, Tianjin University, Tianjin 300072, China, and also with Suzhou Opto-ring Company Ltd., Suzhou 215123, China (e-mail: zhihong.li2007@163.com).

Z. Meng is with the Key Laboratory of Optoelectronics Information Technology Polarization Research Center, College of Precision Instrument and Optoelectronics Engineering, Ministry of Education, Tianjin University, Tianjin 300072, China (e-mail: tjictom@126.com).

L. Wang is with the College of Precision Instrument and Opto-Electronics Engineering, Tianjin University, Tianjin 300072, China, and also with the College of Automobile and Transportation, Tianjin University of Technology and Education, Tianjin 300222, China (e-mail: longzhi_wang@sina.com).

T. Liu is with the College of Precision Instrument and Opto-Electronics Engineering, Tianjin University, Tianjin 300072, China, and also with the Key Laboratory of Opto-Electronics Information Technical Science, Ministry of Education, Tianjin University, Tianjin 300072, China (e-mail: tgliu@tju.edu.cn).

S. X. Yao is with the College of Precision Instrument and Opto-Electronics Engineering, Tianjin University, Tianjin 300072, China, the Key Laboratory of Opto-Electronics Information Technical Science, Tianjin University, Ministry of Education, Tianjin 300072, China, and also with General Photonics Corporation, Chino, CA 91710 USA (e-mail: steveyao888@yahoo.com).

Color versions of one or more of the figures in this letter are available online at http://ieeexplore.ieee.org.

Digital Object Identifier 10.1109/LPT.2014.2384837

pinpoint the location of poor wound sections beneath surface of the fiber coil.

Optical coherence tomography (OCT) is a relatively new imaging technique for detecting the internal microstructures of a sample and obtaining its tomographic images with high spatial resolution. It is most widely used for medical applications, such as those in ophthalmology [10], [11], cardiovascular disease diagnosis [12], dentistry [13], dermatology [14], endoscopy [15], blood glucose monitoring [16], and diagnosis of bronchus [17] and macular problems [18]. Recently, OCT has also been applied to industrial applications to exploit its advantages of being noninvasive, high speed, and 3-dimensional [19]–[22].

We believe OCT is particularly suited for the quality inspection of fiber coils, because its inherent advantages can be well utilized to characterize fiber coils. First, a fiber coil is generally made by layers of optical fibers with diameters ranging from 100 to 250 microns. Such a layered structure is most easily analyzed with tomographic images obtained by OCT. Each fiber layer under coil's surface can be clearly viewed and each fiber in each layer can be inspected individually. Other tomographic imaging techniques, such as X-ray computerized tomography (CT), may not have sufficient spatial resolution. Second, a fiber coil may also contain adhesives surrounding each turn of optical fiber, with an index refraction and a scattering coefficient different from those of the fiber. OCT images therefore can clearly identify the interfaces between the fiber turns and the adhesive, and detect any winding defects. Finally, all tomographic images can be reconstructed into a three dimensional (3D) images to be viewed at different angles and different sections of viewer's choice, making the visual inspection more user friendly.

In this letter, we report what we believe the first experimental study of using OCT to qualitatively evaluate the quality of fiber optical gyroscope coils. We show how to obtain different OCT images of a fiber coil in experiments and demonstrate the ability of using OCT images to visualize the conditions of fibers in different layers for identifying winding anomalies. We then discuss how to implement the OCT inspection technique for fiber coil production and quality insurance. Finally, we discuss the limitations of current OCT system and area for improvement. We believe that OCT inspection can be a useful tool for the production of quality fiber coils.

II. Principle

Fig. 2 shows the experimental setup for obtaining OCT images of a fiber coil. We use a commercial swept source OCT (SSOCT) system from Thorlabs with performance parameters shown in Table I to perform the experiments. A 3D reconstruction software was developed for the OCT system to allow the user to visualize data with different viewing angles and perspectives, with the flexibility of selecting proper experimental parameters, such as the lateral scanning range, the step width and the data sets to be accessed off-line for further image processing and data analysis. In the experiment, we selected a lateral scanning range of 8 mm and a step size of 25μm. As shown in Fig. 2a, the center axis of the fiber coil is affixed to the spindle of a lathe or a fiber winding machine, rotating slowly for a complete rotation at constant rate of 1 rpm, while the OCT probe beam is scanned back and forth rapidly along the X axis at a high speed about 100mm/s. Such a slow rotation rate, combined with the high scanning speed, assures that 1) the whole coil surface can be scanned when the coil completes a 360-degree rotation, 2) each cross section view of the coil is in the XZ plane with a negligible tilting angle of 0.12 degrees, as shown in Fig. 2, and 3) the resolution of the resulting OCT image is not compromised.

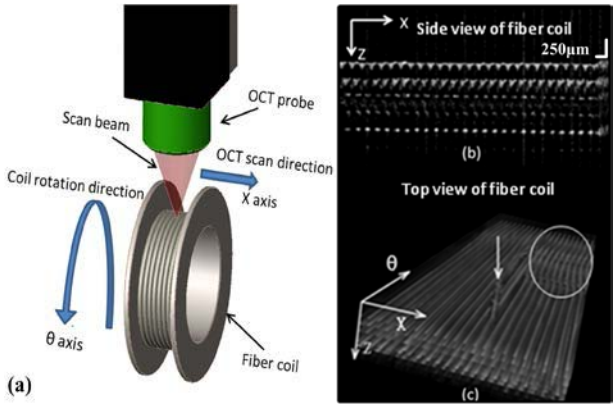

Fig. 2. (a) Illustration of OCT image acquisition of a fiber coil. The fiber coil is affixed on a spindle of a lathe or a winding machine, and is rotated along its center axis at a fixed speed. The probe of the OCT system is above the fiber coil. X axis is the OCT scan direction and θ axis is the rotating direction of the fiber coil. (b) The 2D tomographic image of the coil along the X axis. (c) The reconstructed 3D OCT image of a four-layer fiber coil without adhesive.

TABLE I
Performance Parameters of the Swept Source OCT, Assuming an Index of Refraction of 1.5 in Fiber

Wave-length, μm	1325
Spectral bandwidth, nm	100
Axial Resolution (Air/Fiber), μm	12/8
Transverse Resolution (Air), μm	25
Axial scans rate, KHz	16
Maximum transverse scan rate, mm/s	100
Max. lateral scanning range, mm	10
Maximum image depth (Air/Fiber), mm	3/2

Fig. 2b shows a typical 2D tomographic image obtained by the setup and Fig. 2c shows the reconstructed 3D OCT image when the fiber coil makes one complete rotation (360 degrees). By using the setup and process described above, the circular fiber coil can be viewed as a rectangular volumetric image after 3D reconstruction is performed, making it more convenient for the viewer to identify fiber winding defects inside the fiber coil. In Figs. 2b and 2c, the dark areas are locations of optical fibers because of their weak scatting while the white areas are the interfaces of the fiber and air. In Fig. 2c, a fiber climbing defect marked with a white arrow and the non-uniform fiber turns marked with a white circle are clearly identified.

III. Experimental Results and Discussion

Defects invisible to video inspection can be clearly seen by OCT tomographic images. For example, the non-uniform

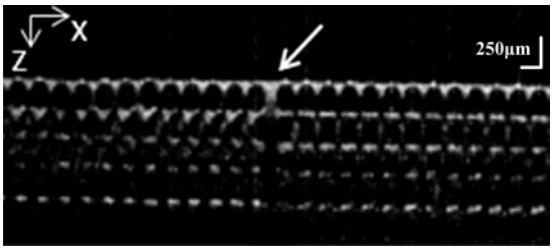

Fig. 3. OCT tomographic image taken during the winding process of a 4-layer fiber coil with potting adhesive, where the low scattering fiber appears dark while the adhesive appears grey or white due to large scattering.

adhesive potting often occurs in a fiber coil, which may affect the thermal performance of the resulting FOG. Fig. 3 shows an OCT image of a 4-layer fiber coil with 200 μm coating fiber. At the location pointed with a white arrow, a defect of excessive adhesive can be clearly identified, because the fiber and the adhesive have different scattering coefficients and contrast sharply in OCT images. On the other hand, such a defect is not visible in a CCD image because the surfaces of both the fiber and the adhesive appear the same and no information below the surface is available.

In Fig. 3, the interfaces between the fiber and the adhesive appear to be white and can be easily visualize due to strong light scattering, while the body of the fiber appears dark in the absence of light scattering. We can also see that the adhesive region with strong scattering (pointed with a white arrow) diminishes the light beneath it and casts a shadow. Such a "shadowing" effect generally prevents the formation of clear OCT images of morphological features in the shadow. This disadvantage can be eliminated by the OCT derivative image which enhanced the morphological features beneath the shadow [23]. On the other hand, as the axial scanning depth increased, the images become less clear due to the strong attenuation of light in the adhesive with less light reaching lower layers. An image enhancement algorithm may be used for improving the image quality in the deep regions [24].

Using the 3D reconstruction software, we obtained the 3D image of the coil with 6 layers. Figs. 4a to 4f show different views of the obtained 3D image. In the figures, the dark areas represent the location of fiber due to its low scattering, while the white areas represent the locations of potting adhesives because of the relative large scattering. In Figs. 4a and 4b, the six layers of fibers are clearly recognized. We believe that the imperfect fiber placements (the lumps and humps) in the upper layers may actually introduce phase distortion and affect the image of fiber arrangements in the lower layers. Therefore some of the apparent winding quality degradation in the lower layers may come from such image distortions introduced from upper layers, which can be compensated in software. Nevertheless, winding defects, such as the concavo-convex defect or fiber overlapping defect in layer 3, can be still clearly identified with the top and side views, as shown in Figs. 4d and 4f marked with red circles. For comparison, the fiber in Fig. 4e are mostly parallel, but is bent in Fig. 4f, probably caused by the squeezing action from other fiber

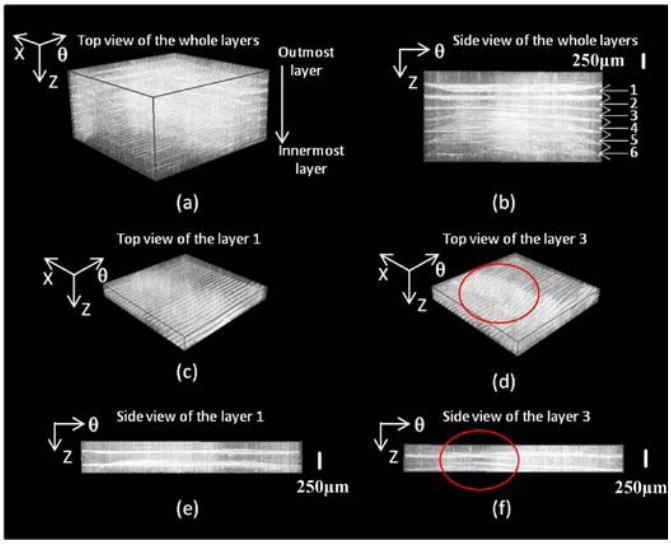

Fig. 4. 3D OCT images of a six-layer fiber coil. (a) volumetric view of a section with all six layers; (b) side view of (a); (c) top view of the top layer with parallel fiber lines; (d) top view of the 3rd layer with defective curved fiber lines; (e) and (f) are the side views of the (c) and (d), respectively.

layers or the irregularity of the fiber diameter. Therefore, by viewing the OCT image from different angles, in different layers, or at different cross sections, one can conveniently identify different winding defects in the fiber coil.

We anticipate this OCT inspection method can be applied to both online (while the coil is being wound on the winding machine) and offline (after the winding is completed) inspections of fiber coils. During fiber winding, the non-uniform pressure or force from the top layers may distort the fiber arrangement in the layers below. With OCT online inspection, not only one can see the winding condition of the top layer, but also whether and how winding a new fiber layer affects the layers below, a capability not attainable with video online inspection. If defects are found, the operator can unwind and rewind the related layers. For this application, imaging 2 to 4 fiber layers is generally sufficient. Our current OCT system has an effective imaging depth about 3 mm in air (2 mm in fiber with an index of refraction of 1.5), limited mainly by the coherence length of the swept-wavelength source and the focusing optics of the probe. Therefore it can obtain images of up to 8 layers of fibers with a coating diameter of 0.25 mm and 12 layers of fibers with a coating diameter of 0.165 mm.

For offline inspection, a quality inspector can evaluate all fiber layers using an OCT system in Fig. 2. Fiber coils with a total number of layers from 8 to 32 are common in practice and the imaging depth up to 5.4 and 8 mm in air may be required for fibers with coating diameters of 0.165 and 0.25 mm, respectively. However, our current OCT system only has an imaging depth of 3 mm in air. One may improve the depth range of an OCT system by 1) increasing the laser coherence length, 2) increasing the Rayleigh range of the probe beam with a proper optic design, and 3) implementing an image enhancement algorithm in the software for lower layers [24]. We are developing software to remove the image distortion in lower layers caused by upper layer winding imperfections.

IV. Conclusion

In conclusion, we propose and demonstrate a novel approach to inspect the quality of fiber coils in both online and offline applications by using OCT. Winding defects in both the top and inner layers can be really identified with the tomographic OCT images. With the aid of a 3D reconstruction software, a fiber coil can be viewed from different angles, at different sections, or in different layers of viewer's choice, making it very convenient to identify, record, and show to others any defects in the coil. We anticipate that the proposed OCT fiber coil inspection method has the potential to become a very useful tool to improve the production quality of the fiber gyroscope coils.

References

[1] V. Vali and R. W. Shorthill, "Fiber ring interferometer," *Appl. Opt.*, vol. 15, no. 5, pp. 1099–1100, 1976.

[2] M. Chomát, "Efficient suppression of thermally induced nonreciprocity in fiber-optic Sagnac interferometers with novel double-layer winding," *Appl. Opt.*, vol. 32, no. 13, pp. 2289–2291, 1993.

[3] R. B. Dyott, "Reduction of the Shupe effect in fibre optic gyros; the random-wound coil," *Electron. Lett.*, vol. 32, no. 23, pp. 2177–2178, Nov. 1996.

[4] R. P. Goettsche and R. A. Bergh, "Trimming of fiber optic winding and method of achieving same," U.S. Patent 5 528 715, Jun. 18, 1996, pp. 6–18.

[5] F. Mohr, "Thermooptically induced bias drift in fiber optical Sagnac interferometers," *J. Lightw. Technol.*, vol. 14, no. 1, pp. 27–41, Jan. 1996.

[6] D. M. Shupe, "Thermally induced nonreciprocity in the fiber-optic interferometer," *Appl. Opt.*, vol. 19, no. 5, pp. 654–655, 1980.

[7] Z. Li, Z. Meng, T. Liu, and X. S. Yao, "A novel method for determining and improving the quality of a quadrupolar fiber gyro coil under temperature variations," *Opt. Exp.*, vol. 21, no. 2, pp. 2521–2530, 2013.

[8] T. De Fazio, K. L. Belsley, R. H. Smith, G. B. Shank, Jr., and W. H. Culver, "Development issues for automating quadrupole-pattern optical-fiber coil-winding for fiber-optic gyro manufacture," in *Proc. IEEE Int. Conf. Robot. Autom.*, May 1994, pp. 202–207.

[9] M. Ivancevic, "Quadrupole-wound fiber optic sensing coil and method of manufacture thereof," U.S. Patent 4 856 900, Aug. 15, 1989.

[10] D. Huang *et al.*, "Optical coherence tomography," *Science*, vol. 254, no. 5035, pp. 1178–1181, 1991.

[11] W. J. Choi *et al.*, "Phase-sensitive swept-source optical coherence tomography imaging of the human retina with a vertical cavity surface-emitting laser light source," *Opt. Lett.*, vol. 38, no. 3, pp. 338–340, 2013.

[12] G. J. Ughi, T. Adriaenssens, W. Desmet, and J. D'hooge, "Fully automatic three-dimensional visualization of intravascular optical coherence tomography images: Methods and feasibility *in vivo*," *Biomed. Opt. Exp.*, vol. 3, no. 12, pp. 3291–3303, 2012.

[13] Z. Meng *et al.*, "Measurement of the refractive index of human teeth by optical coherence tomography," *J. Biomed. Opt.*, vol. 14, no. 3, p. 034010, 2009.

[14] C. Blatter *et al.*, "*In situ* structural and microangiographic assessment of human skin lesions with high-speed OCT," *Biomed. Opt. Exp.*, vol. 3, no. 10, pp. 2636–2646, 2012.

[15] Y. Pan, H. Xie, and G. K. Fedder, "Endoscopic optical coherence tomography based on a microelectromechanical mirror," *Opt. Lett.*, vol. 26, no. 24, pp. 1966–1968, 2001.

[16] Y. Su, Z. Meng, L. Wang, H. Yu, and T. Liu, "Effect of temperature on noninvasive blood glucose monitoring *in vivo* using optical coherence tomography," *Chin. Opt. Lett.*, vol. 12, no. 11, p. 111701, 2014.

[17] S. Lam *et al.*, "*In vivo* optical coherence tomography imaging of preinvasive bronchial lesions," *Clin. Cancer Res.*, vol. 14, pp. 2006–2011, Apr. 2008.

[18] S. Wolf and U. Wolf-Schnurrbusch, "Spectral-domain optical coherence tomography use in macular diseases: A review," *Ophthalmologica*, vol. 224, no. 6, pp. 333–340, 2010.

[19] R. Su, M. Kirillin, P. Ekberg, A. Roos, E. Sergeeva, and L. Mattsson, "Optical coherence tomography for quality assessment of embedded microchannels in alumina ceramic," *Opt. Exp.*, vol. 20, no. 4, pp. 4603–4618, 2012.

[20] K. Fujiwara and O. Matoba, "High-speed cross-sectional imaging of valuable documents using common-path swept-source optical coherence tomography," *Appl. Opt.*, vol. 50, no. 34, pp. H165–H170, 2011.

[21] D. Stifter, "Beyond biomedicine: A review of alternative applications and developments for optical coherence tomography," *Appl. Phys. B*, vol. 88, no. 3, pp. 337–357, 2007.

[22] P. Targowski and M. Iwanicka, "Optical coherence tomography: Its role in the non-invasive structural examination and conservation of cultural heritage objects—A review," *Appl. Phys. A*, vol. 106, no. 2, pp. 265–277, 2012.

[23] L. Z. Wang, "OCT based studies of skin features and their applications in the non-invasive blood glucose test," Ph.D. dissertation, College Precision Instrum. Opto-Electron. Eng., Tianjin Univ., Tianjin, China, 2013, pp. 41–46.

[24] L. Z. Wang *et al.*, "An optical coherence tomography attenuation compensation algorithm based on adaptive multi-scale retinex," *Chin. J. Lasers*, vol. 40, no. 12, pp. 1204001-1–1204001-6, 2013.